UC Berkeley
UC Berkeley Previously Published Works

Title

One-dimensional-shaped MFI-type zeolites for catalytic upcycling of polyurethanes: A combined experimental and density functional theory study

Permalink

https://escholarship.org/uc/item/7vr7336s

Journal

Chemical Engineering Journal, 549

ISSN

1385-8947

Authors

Shikhaliyev, Kanan
Onsree, Thossaporn
Abdullayev, Yusif
et al.

Publication Date

2026-12-01

DOI

10.1016/j.cej.2026.182585

Peer reviewed

eScholarship.org Powered by the California Digital Library
University of California

Chemical Engineering Journal 549 (2026) 182585

Contents lists available at ScienceDirect

Chemical Engineering Journal

journal homepage: www.elsevier.com/locate/cej

One-dimensional-shaped MFI-type zeolites for catalytic upcycling of polyurethanes: A combined experimental and density functional theory study

Kanan Shikhaliyev [a,d], Thossaporn Onsree [b], Yusif Abdullayev [c,e], Samuel M. Drummond [b], Youngkyu Park [a], Alexander Katz [a], Jochen Lauterbach [b,*]

[a] Department of Chemical and Biomolecular Engineering, University of California Berkeley, Berkeley, USA
[b] Department of Chemical Engineering, University of South Carolina, Columbia, USA
[c] Department of Chemistry, The University of Texas at Austin, Austin, USA
[d] Department of Chemical Engineering, Azerbaijan State Oil and Industry University, Baku, Azerbaijan
[e] Department of Chemistry, Texas A&M University-Texarkana, Texarkana, USA

ARTICLE INFO

Keywords:
Polyurethane upcycling
Catalytic cracking
One-dimensional shaped zeolite
MFI
ZSM-5
Aminolysis
DFT study

ABSTRACT

Polyurethane foam (PUF) was synthesized from commercial polyether polyol and methylene diphenyl diisocyanate (MDI) to provide a representative model polyurethane for chemical upcycling. Due to its crosslinked solid structure, PUF was first liquefied via aminolysis with monoethanolamine (MEA) at 150 °C. Density functional theory (DFT) calculations provided additional insight into the differences in aminolysis observed under nitrogen and air. Excess MEA was subsequently removed by evaporation at 170 °C, and the remaining solution was aged overnight, yielding phase separation into a polyol-rich fraction (PRF) and 4,4′-methylenedianiline (MDA) rich phase. While the MDA-rich phase is typically treated as a byproduct, it can serve as a precursor for MDI. The PRF was then catalytically cracked over zeolite catalysts to produce value-added chemicals. A novel one-dimensional (1D) shaped H-MFI zeolite nanorod with enhanced external surface area and mesoporosity may contribute to interactions between polymers and catalysts. Compared to commercial H-ZSM-5, 1D-H-MFI exhibited higher selectivity toward propionaldehyde (61.8 wt% vs. 50.3 wt%) with 50% lower catalyst loading. This two-step strategy demonstrates the potential to upcycle commercial PUF into valuable chemicals.

1. Introduction

For a more sustainable future, polymer waste must be recycled or upcycled. In this field, polyurethanes (PU) present a unique problem. About 25 million metric tons of polyurethane were produced in 2022, and it is forecast to reach 30 million metric tons annually by 2030 [1]. PU is used in a variety of products, including elastomers, coatings, and stiff and flexible foams [2]. Instead of being recycled, around 70% of manufactured polyurethanes are burned or dumped in landfills [3]. Remarkably, more than 70% of all polyurethanes are produced as foams, either in rigid or flexible forms [4]. Unlike many other polymers, such as polyethylene, polystyrene, and polypropylene, polyurethane foams (PUFs) have a complex chemistry that incorporates oxygen in addition to carbon and hydrogen. Because of the oxygen, PU lacks a traditional melting point, making conventional heat-based recycling methods impractical [5]. Instead of producing a reusable fundamental material, heating PUFs causes them to disintegrate into a complex array of chemicals. This makes upcycling particularly challenging. The process of chemically upcycling waste polymers involves a series of steps that break down or depolymerize them into usable monomers. To improve control over reaction rates and selectivity, catalysts can be used. The majority of polymer waste is solid, which makes it difficult for catalysts and polymers to interact, particularly when solid catalysts are used [6].

Liquefying polymers is a common technique to increase contact and interaction. Even without a catalyst, PUFs can break down into a variety of chemicals when heated to 120 °C or above. Long-chain waxes are one class of chemical components commonly produced by the breakdown of PUFs, and reduce the process's profitability [7]. Furthermore, prior data show that in the thermal decomposition of oxygenated polymers, the distribution of products is wide, and the products have limited

* Corresponding author.
E-mail address: LAUTERAJ@cec.sc.edu (J. Lauterbach).

https://doi.org/10.1016/j.cej.2026.182585
Received 22 June 2026; Received in revised form 28 September 2026; Accepted 29 September 2026
Available online 30 September 2026
1385-8947/© 2026 The Authors. Published by Elsevier B.V. This is an open access article under the CC BY-NC-ND license (http://creativecommons.org/licenses/by-nc-nd/4.0/).

selectivity [8].

Several methods, including hydrolysis, glycolysis, acidolysis, and amylolysis, have been developed to selectively break down PU bonds [9]. However, apart from impurities and waxes, these methods typically yield polyols and other aromatic derivatives [10]. Therefore, additional reactions are needed to convert these polymeric and/or oligomeric products into usable monomers, increasing the feasibility of PU upcycling. Compared with the original PUFs, these shorter-chain liquid products are easier to process.

A well-studied process called aminolysis shows that monoethanolamine (MEA) can preferentially interact with the urethane groups in PUFs, releasing the polyol component while forming a bond with the 4,4′-Methylenedianiline (MDA) component (when methylene diphenyl diisocyanate (MDI) was used in the original polyurethane foam). MDA-rich phase is formed during this process and then separated from the polyol [11]. PUFs generally consist of 60–70% wt. polyols with additives and aromatic isocyanate-derived as the remaining portion. Polyols, therefore, constitute a significant portion that would be obtained through aminolysis. In other words, to develop an upcycling process for waste PUFs, it is necessary to produce value-added chemicals from the polyol fraction. Due to impurities and structural differences in the raw ingredients, the previously synthesized polyols used to produce polyurethane foams are not particularly beneficial. As a result, the polyol fractions that are produced have varying molecular weights and compositions, especially when it comes to the proportions of two-carbon to three-carbon components [12]. Usually made from propylene and ethylene oxide, these polyether polyols consist of two- and three-carbon monomers [13]. Additionally, homopolymer monomers such as polyethylene glycol (PEG) and polypropylene glycol (PPG) can be synthesized from epoxides. Propionaldehydes can be produced with high selectivity using H-ZSM-5 type zeolites, according to research on the catalytic breakdown of PPG [8]. Compared to more complex polymers like PUF, it is easier to improve product selectivity because they share the same repeating 3-carbon chain. Nonetheless, catalytic cracking reactions encounter numerous diffusion constraints due to the substantial molecular sizes of the polymers. Zeolites, when used as catalysts, often possess extensive surface areas; however, a significant portion of this surface area arises from their microporous regions, which are inaccessible to high-molecular-weight polymers. The outer and mesoporous surfaces of the zeolites are where these interactions primarily occur between zeolites and polymers. To reduce non-catalytic events and increase catalyst interactions with reactants, it is essential to increase the mesoporosity of zeolites used in the catalytic breakdown of polymers [14]. There are many ways to increase external surface area, which can be broadly divided into two categories: one is post-synthesis modification of zeolites using methods like dealumination and desilication [15]. A different approach is to modify the synthesis procedure, particularly by employing specific surface-directing agents. Temperature, concentrations, and process length are examples of synthesis parameters that have an impact on zeolite surface shape [16].

In this work, one-dimensional (1D) shaped MFI-type zeolites are synthesized by modifying the synthesis procedure. Those zeolites are called 1D-shaped because of their rod-like shapes and their thicknesses being significantly smaller than their lengths. In this study, PUFs were reacted with MEA to produce at least two different layers: (i) one of which was enriched in the polyol component of polyurethane foam and (ii) the other of which was primarily composed of products originating from the MDI component. The primary component, which is the polyol-rich fraction, was selected for further processing.

Furthermore, to understand the chemistry of the aminolysis of PUFs, DFT simulations were conducted to identify potential products and analyze the possible influence of air on the decomposition process.

The next step involved applying the knowledge gathered from the catalytic breakdown of oxygenated polymers with zeolites. This was done to utilize high external surface area, one-dimensional mesoporous zeolites to upcycle the polyol-rich fraction of polyurethane foams into high-value chemicals. To improve the target product selectivity, the reactor architecture, zeolites, and reaction conditions were investigated. To provide highly active and selective zeolites as catalysts for the process, specialized 1D-shaped zeolites were created, and the synthesis method was optimized. A previously described Gemini cationic surfactant was used as a surface guiding agent in the zeolite synthesis process, and the surfactant was applied to create two-dimensional, flower-like zeolites [17]. However, in this work, the synthesis process was optimized to develop one-dimensional, nano-rod-shaped zeolites.

2. Materials and methods

2.1. Materials

Commercial methylene diphenyl diisocyanate (MDI) and polyether polyol (average MW of 1500) were employed to synthesize a PUF. Polypropylene glycol (M_W of 425 g/mol) and polyethylene glycol (MW of 8000) were purchased from Fisher Scientific. NH_4-ZSM-5, with a SiO_2/Al_2O_3 molar ratio of 80:1, was purchased from Alpha Aesar and calcined at 580 °C for 4 h to convert the ammonium form of zeolite to the hydrogen form (H-ZSM-5).

2.2. Synthesis of polyurethane foams and starting materials

Commercial polyether polyol (polyol) and MDI (isocyanate) were utilized as starting materials for a PUF. The mixing ratio of polyol to isocyanate was 2:1 by weight. The molecular weight of pure polyether polyol was analyzed by MALDI (Supplementary Fig. S1). MDI primarily consists of monomers with an average molecular weight of approximately 250 g/mol. Polyol and isocyanate were mixed at room temperature for 15 s, then left for an hour to yield a PUF.

2.3. Preliminary decomposition of solid PUF to liquid products

Because the produced PU is a solid foam, catalytic processes involving solid catalysts are difficult. Therefore, the foams were liquefied by using aminolysis reaction. The aminolysis process, which replaces the polyurethane carbonylic carbon with an amine group. According to Kanaya and Takahashi, liquid products are produced when polyurethane and MEA react at 150 °C in air under stirring and no catalyst [11]. A three-neck glass reactor equipped with a condenser was used to carry out the process, allowing the condensation of evaporated MEA. Furthermore, the reaction was carried out under nitrogen and as well as air mixture. More detailed observations and conditions, of the air-nitrogen mixture, are provided in the Supporting Information (SI). As aminolysis was used primarily as a tool to separate PRF from the PU foam in this study, the effect of air flow (or air concentration) was not systematically investigated. However, the influence of air on PU decomposition has been experimentally investigated in prior work [18]. After the reaction, the temperature was increased to 170 °C without the reflux line to remove MEA by evaporation.

After the reaction, the products were left in the flask overnight, which caused the liquid to separate into layers. According to ^{1}H NMR data, the lower layer is rich in 4,4-Methylenedianiline (MDA-rich), while the upper layer is a polyether polyol-rich fraction (PRF) (Supplementary Fig. S2). Better control over product selectivity is achieved by creating two distinct layers and separating them, thereby enabling two distinct reactions. A broader product spectrum and reduced product selectivity would result from combining the two phases and reacting them. It is noted that the polyol-rich top layer contained a few impurities of aromatics, and there were also some polyol impurities in the MDA-rich lower layer. In addition, the ^{1}H NMR results (Fig. S6) show that significant amounts of MDI and MEA are also present in the MDA-rich phase, which is consistent with previously reported literature [19].

2.4. Computational details

To theoretically investigate the reaction between PUF and MEA, the Gaussian 16 software package was used for calculations [20]. All species (reactants, intermediates, and transition state (TS) structures) were optimized without geometry constraints using Kohn-Sham Density Functional Theory (KS-DFT) and the B3LYP functional with D3BJ dispersion corrections [21,22]. These are reasonable for an accurate assessment of energy barriers for organic molecules [23]. The 6-31G* basis set was used for all atoms (H, C, O, and N). Since the polymer decomposition reaction was carried out at a high temperature (150 °C), the gas phase was considered for all calculations. PUF was substituted in the calculations as C_6H_5-CH_2-C_6H_4-NH-C(O)-O-CH_2-CH_2-OH (repeating unit), simplified PUF fragment to avoid computational overhead. This substitution reasonably represents PUF, as the focus of the computation is urethane (carbamate) bond cleavage with MEA. Minima (0 imaginary frequency), saddle points (1 imaginary frequency), and free energies were identified via frequency calculations. Intrinsic reaction coordinate (IRC) searches were employed to identify related intermediates and products associated with the transition states (TS). Total energies, Gibbs energies, enthalpies, and optimized geometries (in xyz format) of all structures were included in the Electronic Supplementary Information (ESI).

2.5. Analysis methods of polymers

Polymers were analyzed by ^{1}H NMR recorded on a Bruker AVANCE III-HD 400 spectrometer operating at 400 MHz, using deuterated methanol and acetone as solvents. Matrix-assisted laser desorption/ionization (MALDI) mass spectra were acquired on a Bruker rapifleX time-of-flight spectrometer, utilizing α-Cyano-4-hydroxycinnamic acid as a matrix and acetone (and methanol) as solvents.

2.6. Synthesis of 1D-shaped MFI type zeolites

Beginning with the preparation of the organic structure-directing agent (SDA), a Gemini cationic surfactant with the structure [$C_{22}H_{45}$-$N^+(CH_3)_2$-C_6H_{12}-$N^+(CH_3)_2$-C_6H_{13}] Br_2 ($C_{22\text{-}6\text{-}6}$), as documented in the literature [17], the synthesis of 1D-shaped MFI-type zeolites was initiated. $55K_2O/1Al_2O_3/100SiO_2/10$ $C_{22\text{-}6\text{-}6}/3500H_2O/19H_2SO_4$ was the ratio used to create the zeolites, which were then hydrothermally produced for five days at 170 °C while being stirred at 50 rpm using a magnetic stir bar. In order to create K-MFI zeolite, the zeolites were first cleaned with deionized water until they reached a neutral pH, then centrifuged to separate the particles, dried at 80 °C for 10 h, and then calcined at 550 °C for 4 h under air to eliminate surfactants and other volatile species. Following ion exchange with a 1 M ammonium nitrate solution, the zeolite was converted to its ammonium form. It was then dried for 10 h at 80 °C and calcined for 4 h at 580 °C to obtain the hydrogen form, or H-MFI. During crystallization, the surfactant C22-6-6, which has two cationic heads, was essential in guiding the structure and changing the final product's surface composition. To improve the interaction between crystallites and the SDA, zeolites were synthesized hydrothermally in rotary autoclave ovens. Many variables, including chemical concentrations, temperature, duration, stirring speed, pH, and the order of addition, can be adjusted during synthesis to produce a variety of morphologies with the same SDA. The SiO_2/Al_2O_3 ratio was kept at 100:1 in this investigation, and further synthesis parameters were adjusted to create 1D-shaped zeolite forms, or 1D-H-MFI, where H stands for the final zeolite's hydrogen form. The hydrogen form of the zeolite, known as H-ZSM-5, was also produced by calcining commercial ZSM-5 in ammonia form for 4 h at 580 °C, containing a SiO_2/Al_2O_3 ratio of 80:1. Spent catalysts were calcined at 550 °C for 4 h under air to remove coke for the reusability test.

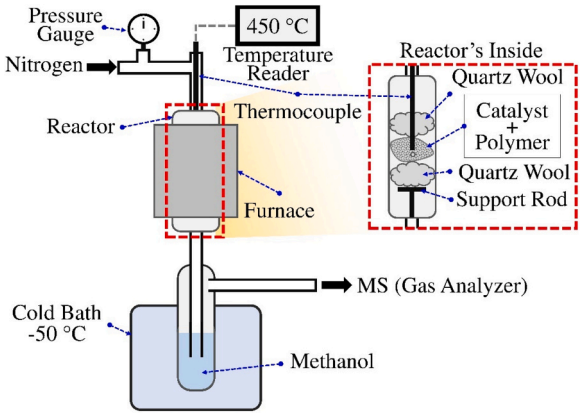


Fig. 1. Schematic setup of the liquefied polymer upcycling reactor.

2.7. Experimental setup for catalytic upcycling of PRF

The custom-built reactor system, a modified version of a previously published arrangement [14], is shown in Fig. 1. In the previous study, nitrogen flowed in an upward direction with products removed from the reactor at the top. However, due to heavy wax production, the flow in this study was reversed and nitrogen was flowed in a downward direction, allowing the wax to flow with the nitrogen. After the reactor, the products were collected in a cold methanol trap for analysis.

To maintain a constant reactor temperature, heating tape was used to raise the nitrogen inlet line to 200 °C. A 316 stainless-steel tube, 300 mm long and 12.7 mm (1/2 in.) in outer diameter, was used as the reactor and placed vertically inside a furnace. The reactor exit was reduced to a tube with an outer diameter of 3.2 mm, and it was submerged in methanol chilled by injecting liquid nitrogen. To condense more than 90 wt% of the products into the liquid phase, the methanol was kept at −50 °C. The remaining products either stayed as residues on the catalyst surface or exited the reactor as gas. A support rod made it easier to precisely set the catalyst bed in each experiment. The catalyst bed foundation was created by inserting a piece of quartz wool over the support rod and flattening it. As shown by the red dashed line frame in Fig. 1, a catalyst and polymer combination, typically 1.0 ± 0.1 g, was then introduced to the reactor and covered with another piece of quartz wool to secure the bed in place. To track the reaction temperature, a thermocouple was inserted into the catalyst bed from the top of the reactor.

2.8. Reaction conditions and product analysis

To ensure that the reactants and catalysts remained solid and within the vertical reactor bed, the catalysts were premixed with polymer at mass ratios of 1:1 and 2:1 (see Fig. 1). Because the catalysts and starting materials were similar, the reaction parameters, including nitrogen flow and reaction temperature, were maintained as in earlier studies [8]. The temperature was ramped up from room temperature to the reaction temperature under continuous nitrogen flow throughout the first 7 min of the 30-minute reaction, which was carried out at 450 °C.

Gas chromatography-mass spectrometry (GC–MS) was used to analyze condensed liquid products in methanol at the end of the reaction. A mass spectrometer system with a base pressure of approximately 10^{-10} Torr was also used to analyze the exhaust gas. It was outfitted with a Varian V-250 MacroTorr turbomolecular pump, supported by an Alcatel 2021 SD oil-sealed rotary vane pump, a Kurt J. Lesker Series 979 vacuum gauge, an MDC ULV-150 leak valve, and a Stanford Research Systems RGA-200 mass spectrometer.

An RTX-1701 column mounted on a 2010 Shimadzu gas chromatography–mass spectrometry (GC–MS) system was used to analyze and identify the collected methanol-containing condensed liquid products.

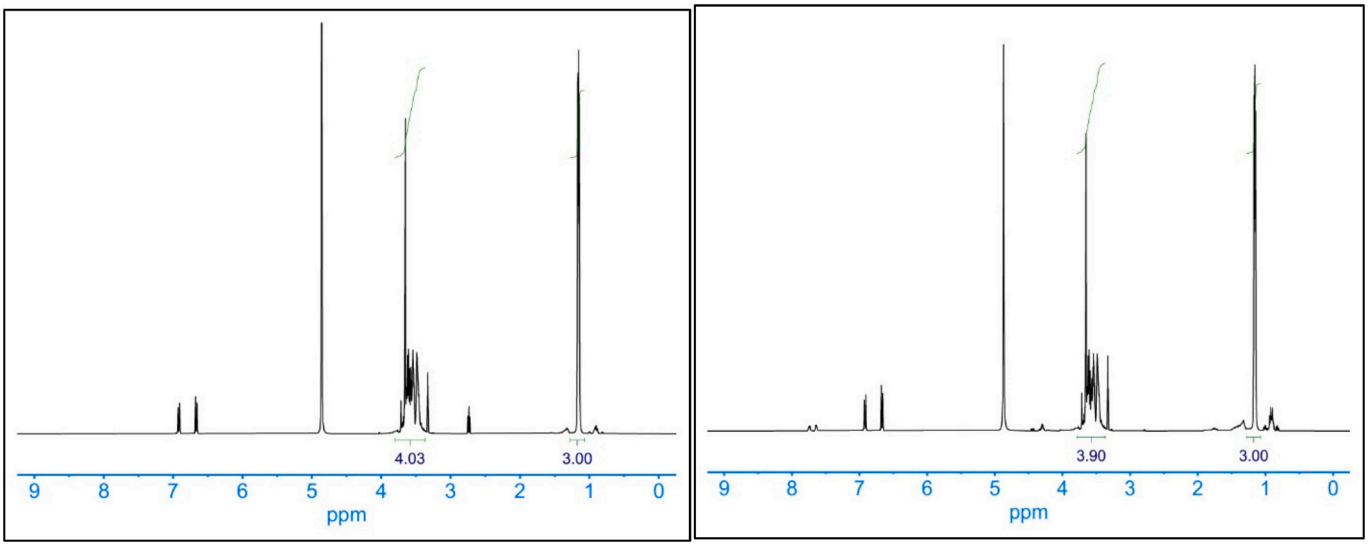


Fig. 2. ^{1}H NMR results: left – pure polyol polyether, right – recovered polyol-rich fraction of PUF.

There was no additional dissolution of the condensed samples in 75 ml of methanol. A split ratio of 10:1 was used to inject 500 nl of each sample into the column. With a steady ramp rate of 20 °C/min, the column temperature was increased from 40 °C for 3 min to 80 °C (held for 2.5 min) and then to 200 °C (held for 5 min). To avoid solvent saturation of the detector, a solvent cut time was introduced. For the remainder of the analysis, MS scanning from 14 to 380 *m/z* commenced at 1.35 min.

The final product mixture contains more than 10 peaks that the GC–MS equipment can identify. Due to the presence of long-chain waxes in certain products, product selectivity was determined using mass fractions, and these products were calibrated using external calibration standards.

2.9. Catalyst characterization

A Rigaku MiniFlex II was used to perform X-ray diffraction (XRD) with Cu Kα source radiation (α = 1.5406 Å). With a step size of 0.02° and a scan rate of 2°/min, each sample was scanned from 2θ = 10° to 80°. Using a Micromeritics ASAP2020 adsorption device, N_2 adsorption isotherms were measured at 77 K. The Barrett-Joyner-Halenda (BJH) method was used to determine the mesopore volume, while the Brunauer–Emmett–Teller (BET) method was used to determine the surface areas and micropore volumes. The acidity of the catalysts was evaluated by temperature-programmed desorption of ammonia (NH_3-TPD) using an Anton Paar Autosorb iQ. Prior to analysis, the samples were pretreated at 550 °C for 1 h under a helium flow. The samples were then exposed to ammonia at 100 °C for 45 min, followed by purging with helium at the same temperature for 45 min to remove non-adsorbed and physisorbed ammonia. Subsequently, the temperature was ramped to 700 °C to desorb the adsorbed ammonia, and the desorbed species were monitored using a thermal conductivity detector (TCD).

The morphologies of the produced zeolites were examined using scanning electron microscopy (SEM) imaging with a Zeiss Gemini500 FESEM. A secondary electron detector (SE2) operating at 15 kV was used for imaging.

For the 1D-H-MFI and H-ZSM-5 catalysts, solid-state ^{27}Al MAS NMR spectra were captured using a Bruker 4 mm MAS probe and a Bruker DSX500 spectrometer. A short rf pulse (0.5 ms-p/18 flip angle) and powerful ^{1}H decoupling pulses were followed by free induction decay signals to describe isolated tetrahedral framework aluminum and extra-framework aluminum (EFAl) constituents within the zeolites. In ambient settings, the sample spinning rate was 13 kHz. For the ^{27}Al nucleus, chemical shifts were externally calibrated using a 1 M $Al(NO_3)_3$ aqueous solution at 0 ppm.

Since the accumulation of carbonaceous elements on the catalyst surface can impair catalytic performance [23–26], coking and organic residues are significant problems in catalytic cracking reactions [23]. Coke accumulation on post-process catalysts can be characterized using various methods. Thermogravimetric (TG) analysis was used in this study. A 2010 Shimadzu TGA-50H, equipped with a GC-60A flow control unit, a BLW-50 cooling blower, and a TA-60WS thermal analysis unit, was used to evaluate the used catalysts. Each used catalyst sample was evaluated at 10 mg. At a fixed heating rate of 10 °C/min, the TG analysis was conducted from room temperature to 600 °C. It was then held at 600 °C for 10 min while air flowed at a fixed rate of 200 ml/min. Every wasted catalyst underwent several tests. Furthermore, the organic residues of PRF on the spent catalyst were examined using ^{13}C MAS NMR. For the ^{13}C nucleus, chemical shifts were externally calibrated using TMS.

3. Results and discussion

3.1. Preliminary decomposition of solid PU foams to liquid products

Commercial MDI and polyether polyol were used to create a PUF. However, the configurations of polyol sections can vary. Thus, ^{1}H NMR and MALDI were used to examine the first polyether polyols. The ^{1}H NMR data are displayed in Fig. 2 (right), where two distinctive peaks of polyether polyols are detected at 1.1 ppm and 3.6 ppm. Certain peaks at 6.5–7 ppm are attributed to aromatic contaminants from polyol additions, such as reaction initiators and fire retardants [24]. Peaks from the deuterated methanol solvent are located at approximately 3.4 ppm and 4.9 ppm. Fig. 2 (left) shows the ^{1}H NMR data for PRF, which are similar, indicating that MEA successfully separated the polyol component from the PUF. Impurities from the MDA-rich fraction were represented by a few additional aromatic peaks that were found between 7.5 and 8 ppm. A crucial feature of polyether polyols is their ratio, since they are made from propylene and ethylene oxides [25]. Ethylene oxide to propylene oxide ratios for pure polyether polyol and PRF are 0.34 and 0.3, respectively, according to calculations based on the polyether polyol's structure [26]. This discrepancy may be due to experimental error or the gas products produced during aminolysis.

The molecular weights of fresh polyether polyol and PRF were also assessed using MALDI; the corresponding findings are shown in Fig. S1. The effective aminolysis of the PUF to polyether polyols is further supported by the fact that both polyols have average molecular weights

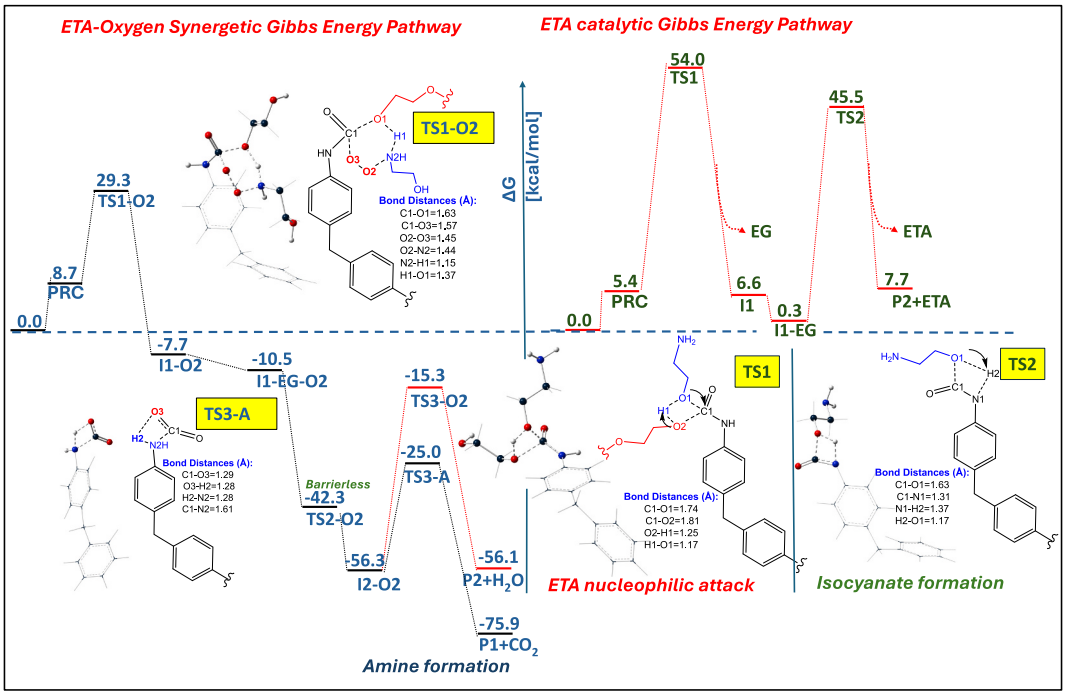


Fig. 3. Energy surfaces for PUF decomposition showing MEA-oxygen synergistic effects (left) versus MEA catalytic effects (right). Important TSs with related bond distances are shown for better understanding of the energy routes. For the intermediate and some TS structures not shown here see ESI and Fig. 5. Some hydrogen and carbon atoms at the TS structures are omitted to avoid clutter.

between 1000 and 2000 amu. The extensive range of random molecular weights in the pure polyether polyol, in contrast to PRF, which shows peaks with a constant difference of 58 g/mol, is another notable difference in the MALDI data. This number is equivalent to the molecular weight of the polyether polyol 3-carbon component, indicating that the polyol component becomes more ordered during polyurethane polymerization. Propionaldehyde and acetone, which have a molecular weight of 58 g/mol, are the products of decomposition that most likely result from C—O bond cleavage. Such possibilities are discussed in the pathway section of the article.

To create useful compounds, the successfully recovered PRF was subsequently used as a liquid feedstock in the catalytic cracking process.

3.2. Computational investigation of initial thermal decomposition of PUFs

Previous studies on the decomposition of PUF into value-added compounds have raised uncertainties regarding the role of MEA [27]. We turned to computational methods to shed light on debates about the roles of the MEA amine and hydroxyl components in PUF cracking. The investigation began with a transition-state search for the MEA amine side attack on the carbonyl carbon of the carbamate functional group. All optimization attempts resulted in unrelated TS structures or failed

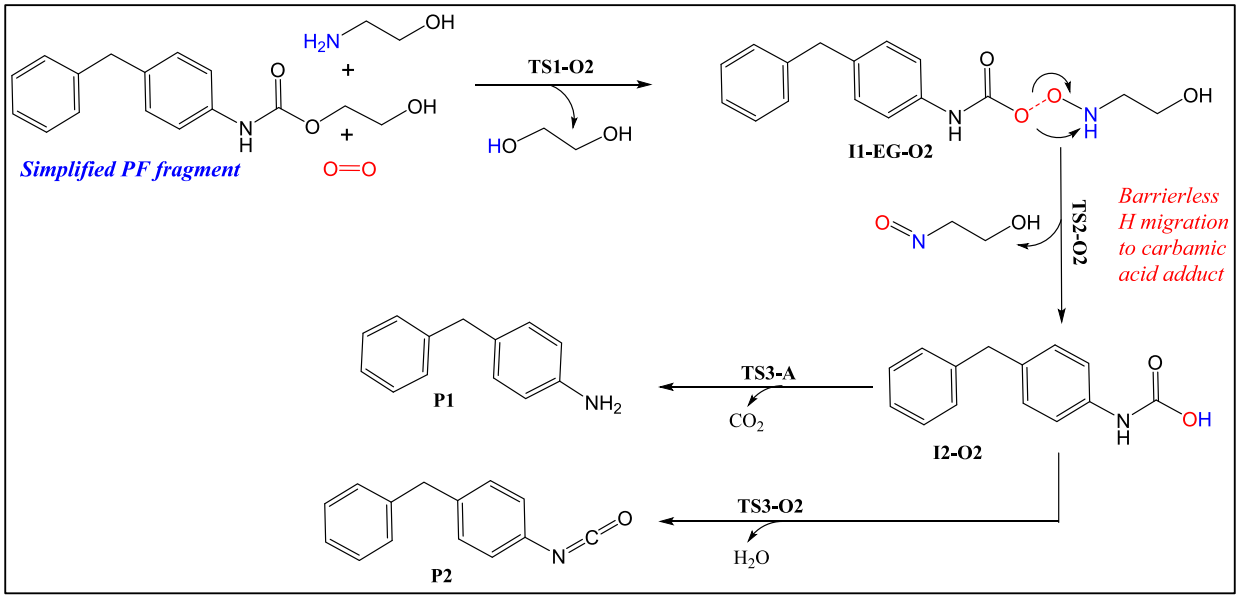


Fig. 4. Calculated reaction route shows the PUF fragment cracking by molecular oxygen and MEA support to amine (P1) and isocyanate (P2) adducts. For TS structures see Fig. 3 and ESI.

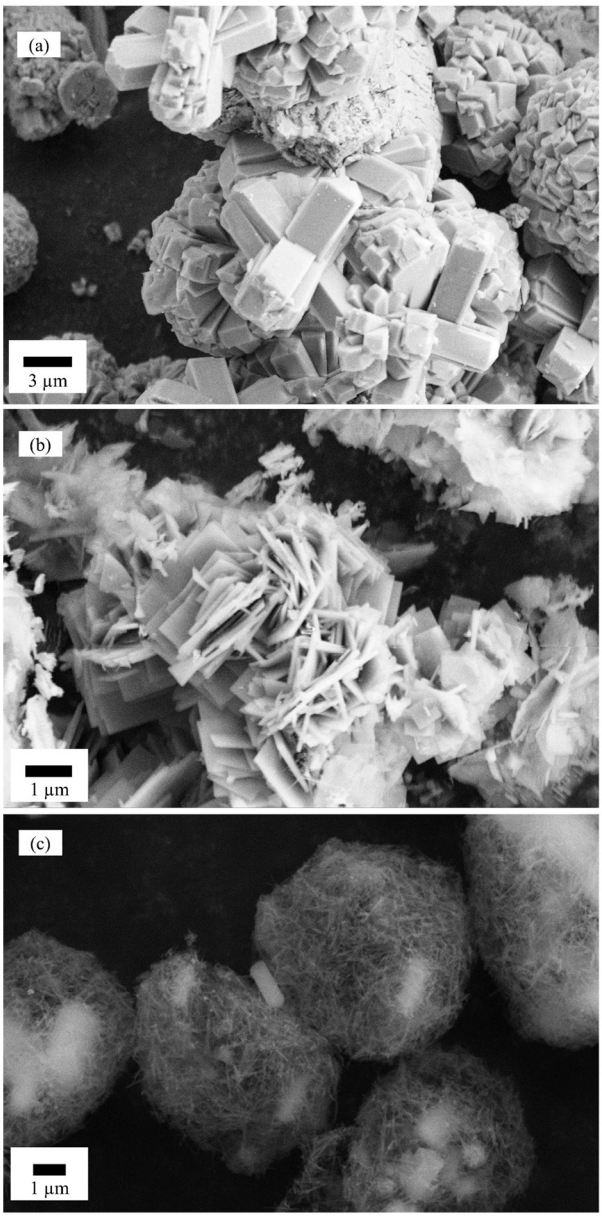


Fig. 5. SEM images of the synthesized MFI-type zeolites crystallized under different conditions.

due to convergence issues. Therefore, an earlier hypothesis was suggested, indicating that PUF cracking is primarily dependent on the nucleophilic attack of the MEA OH side on the carbamate carbonyl.

As shown in Fig. 3, **TS1** represents the possibility of the aforementioned MEA OH (O1) attack on the carbonyl carbon (C1) with a bond distance of 1.74 Å. The associated barrier for **TS1** is calculated to be 54.0 kcal/mol. **TS1** is a concerted TS that leads to the removal of ethylene glycol (EG). **TS2** is calculated to have an energy barrier of 45.2 kcal/mol, leading to MEA termination and the formation of the isocyanate adduct (**P2**). The overall reaction is calculated to be endergonic by 7.7 kcal/mol. The experimental results suggest that airflow may influence PUF cracking and the resulting reaction yield. To identify the role of molecular oxygen in the reaction, one oxygen molecule was included in the starting materials. The calculations show that adding oxygen (**TS1-O2**) reduces the energy barrier by 24.7 kcal/mol compared to **TS1** (MEA catalytic path). The calculated **TS1-O2** involves molecular oxygen cracking (via a 1.45 Å bond distance), with the resulting oxygen atoms (O2 and O3) binding to the MEA nitrogen (N2-O2; 1.44 Å) and the

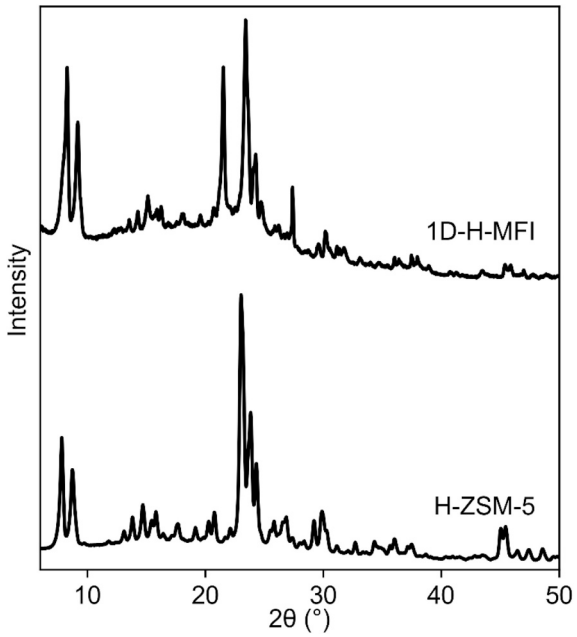


Fig. 6. XRD pattern of H-ZSM-5 (80:1) and 1D-H-MFI (100:1).

carbonyl carbon (C1-O3; 1.57 Å), as shown in Fig. 3. **TS1-O2** yields **I1-EG-O2**, which can convert to **I2-O2** without an energy barrier, as depicted in Fig. 4. Hydrogen migration cleaves the peroxy bond (-O-O-), yielding a carbamic acid adduct (**I2-O2**) and 2-nitrosoethan-1-ol. The computational results showed that further conversion of **I2-O2** to either isocyanate or amine moieties is possible via **TS3-O2** and **TS3-A** TSs. Intramolecular proton migration of H2 to N2 through a 1.28 Å bond distance (TS3-A) results in CO_2 extrusion (C1-N2; 1.61 Å) from the structure. The calculations revealed that the energy barrier for amine adduct formation (**P1**) is 31.3 kcal/mol, which is 11.3 kcal/mol lower than that of **TS3-O2**, which leads to the isocyanate adduct (**P2**).

The opposite intramolecular proton migration from the amine part (N2) to the carboxyl (O3) oxygen yields the isocyanate adduct (**P2**), with an energy barrier of 41.0 kcal/mol. The computational studies are consistent with previous experimental results, indicating the formation of 4,4-methylenedianiline from the decomposition of MEA-supported PUF [11]. Additionally, the analysis revealed the impact of oxygen on PUF cracking by comparing the oxygen-free energy surface (right part of Fig. 3, red energy surface) with the MEA-oxygen synergistic surface (Fig. 4). The downhill exergonic energy surfaces, with −75.9 kcal/mol for the amine adduct (**P1**) and −56.1 kcal/mol for the isocyanate adduct (**P2**), contrast with the endergonic reaction (7.7 kcal/mol) that produces **P1**, highlighting the significant role of oxygen in PUF decomposition.

3.3. *One-dimensional MFI-type zeolites as catalysts*

Initially, 3D shaped MFI structures were synthesized using the same cationic gemini surfactant without stirring and with a SiO_2/Al_2O_3 ratio of 50 (Fig. 5a). Subsequently, the SiO_2/Al_2O_3 ratio was increased to 100, the stirring rate was set to 20 rpm, and the calcination temperature was adjusted to 150 °C, resulting in the formation of 2D-shaped MFI structures (Fig. 5b). Finally, further optimization of the synthesis conditions, as described in the experimental section, led to the successful formation of 1D-shaped MFI structures (Fig. 5c).

Several techniques were used to characterize the synthesized 1D-H-MFI zeolites. Their crystallinity was first verified by XRD. The XRD patterns of the commercial H-ZSM-5 and the produced 1D-shaped zeolites are displayed in Fig. 6. The 1D-shaped zeolites have an MFI-type pattern. Thus, to compare the effects of 1D-shaped and 3D-shaped MFI-type zeolites, commercial H-ZSM-5 with the closest accessible

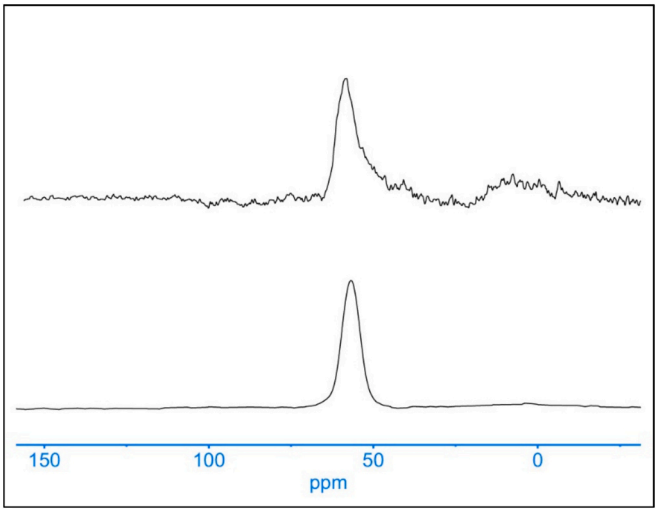


Fig. 7. ^{27}Al MAS NMR results.

SiO_2/Al_2O_3 ratio was used. The majority of the supplied aluminum particles were successfully crystallized and incorporated into the framework, as indicated by 27Al MAS NMR analysis of the resulting zeolites (Fig. 7).

The surface morphology of the zeolites was examined using nitrogen physisorption and SEM. According to Fig. 8 (Fig. S9), the 1D-shaped zeolites are classified as such because of their nanorod-like shape. In comparison to the benchmark H-ZSM-5, the 1D-H-MFI zeolites exhibit much greater surface area and bigger pore volumes, as shown by the nitrogen physisorption analysis (Table 1).

The physical interaction between the catalyst and the polymer was examined using a straightforward assay. As a model polymer, polypropylene glycol (MW 425) was combined with the tested catalysts in varying proportions. The close contact between the polymer and the catalyst was achieved at a 2:1 ratio. Fig. S3 displays 1D-H-MFI and H-ZSM-5 mixed with PPG (MW = 425) at a mass ratio of 2:1. With this quantity of polymer, H-ZSM-5 forms a slurry, whereas 1D-H-MFI absorbs the polymer and remains a solid powder. According to this test, 1D-H-MFI has a significantly larger interaction surface area, which facilitates the polymer's catalytic reaction on these surfaces.

3.4. Catalytic activity of different zeolites in the decomposition of PRF polymers

Prior to the reaction, PRF made from solid PUFs and MEA was combined with various zeolites at a 1:1 (or 2:1) mass ratio and loaded into the reactor tube. After 30 min at 450 °C, the reaction was estimated to have reached full conversion, as no clear evidence of unreacted starting polyol was detected by GC–MS or ^{1}H NMR. Accordingly, full conversion is assumed for the calculations throughout this paper. However, trace amounts of unreacted polyol in the wax fraction cannot be completely excluded. Products were analyzed as liquids after condensation in cold methanol at −50 °C, and gas products were examined by mass spectrometry. The liquid product analysis findings are displayed in Fig. 9. Compared with H-ZSM-5 (80:1), 1D-H-MFI shows greater selectivity for propionaldehyde and lower byproduct selectivity. The catalytic breakdown of polypropylene glycol (PPG), where acetone is mainly generated from the non-catalytic breakdown of polyols, showed a similar pattern [8,28]. Higher acetone selectivity may result from non-catalytic decomposition during the catalytic reaction caused by inadequate catalyst-polymer contact. As previously mentioned, the primary distinction between 1D-H-MFI and H-ZSM-5 lies in their surface morphology; 1D-H-MFI has a substantially larger external surface area, which suggests a possible contribution to interaction between the polymer and the active sites of the catalyst. Using reaction conditions taken from earlier research, the catalytic breakdown of PRF was conducted at 450 °C with nitrogen flow [8]. As 1D-H-MFI contains a lower Al content than H-ZSM-5, the NH_3-TPD results indicate a lower overall concentration of acid sites in 1D-H-MFI (Fig. S5). However, NH_3-TPD probes acid sites within the micropores, including sites that may be inaccessible to PRF due to its larger molecular size. Since the initial cracking of PRF is expected to occur predominantly on the catalyst's external surface, a larger external surface area is critical for initiating cracking. Following the initial conversion, smaller molecular intermediates generated during cracking may diffuse into the micropores, where they can undergo further reactions. These secondary reactions within the micropores may subsequently influence the product distribution and contribute to the observed selectivity toward the final products. Investigations were also conducted into gas products. Table 2 shows the mass balance of solid, liquid, and gas products. According to the analysis, methane, carbon monoxide, and carbon dioxide are present at trace levels in the gas products, which are mostly composed of hydrogen, carbon monoxide and propylene. Such gases can be separated and used in various ways during an industrial-scale upcycling process [29,30].

Table 1
Surface area, pore volume, and pore sizes.

Zeolite name	BET surface area (m^2/g)	External surface area (m^2/g)	Pore volume (cm^3/g)	Average Pore size (nm)
H-ZSM-5 (80:1)	303	112	0.19	2.63
1D-H-MFI (100:1)	360	184	0.31	3.51

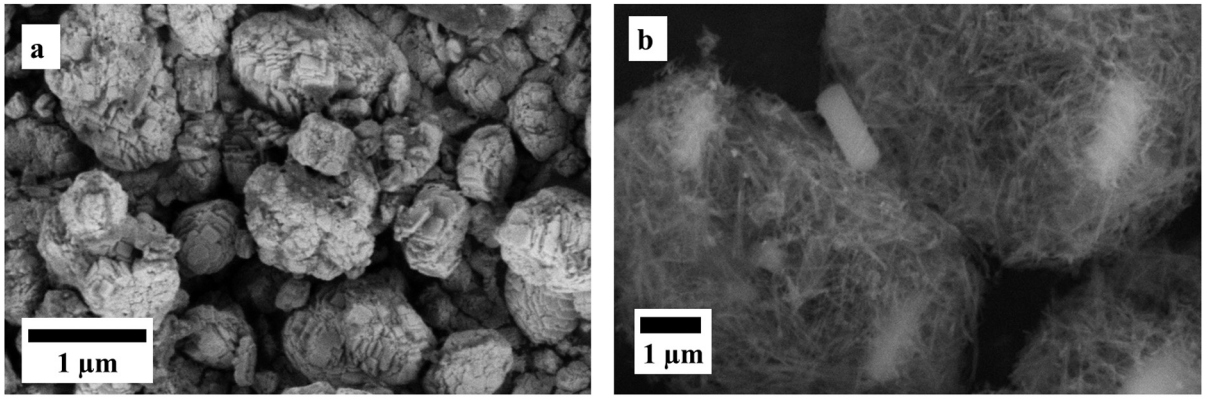


Fig. 8. SEM images of (a) H-ZSM-5 and (b) 1D-H-MFI.

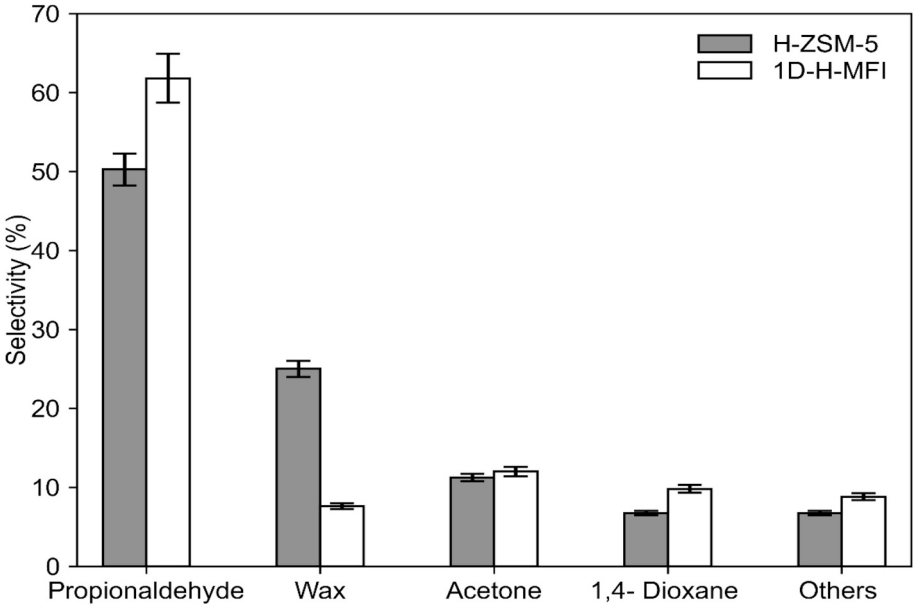


Fig. 9. Liquid product selectivity (wt%) of catalytic cracking of PRF.

Table 2
Product phase distribution.

Catalyst	Gas products (wt%)	Liquid products (wt%)	Solid products (wt%)
H-ZSM-5	4.9	92.3	2.8
1D-H-MFI	3.4	94.4	2.2

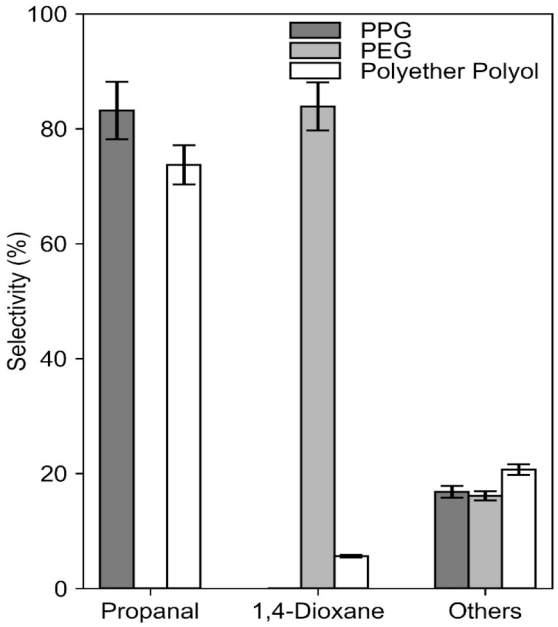


Fig. 10. Liquid product selectivity (wt%) of catalytic cracking of PPG, PEG, and Polyether polyol by using H-ZSM-5 (80:1).

3.5. Characterization of spent catalysts

The spent catalysts had darker appearances with solid residues. The amount and makeup of these residues were examined using TGA and ^{13}C MAS NMR. The solid deposit was 2.2 ± 0.2 wt% for 1D-H-MFI and 2.8 ± 0.3 wt% for H-ZSM-5. Long-chain and aromatic hydrocarbons trapped in the zeolite pores make up the majority of the deposits, according to ^{13}C MAS NMR studies. According to several reports, coking is increased when the zeolite's aluminum content is raised [31,32]. Because fewer hydrocarbons become caught on the surface, 1D-shaped zeolite's increased mesoporosity may help reduce residue development. The amount of solid deposits on the zeolite may also be influenced by the slightly reduced aluminum content of 1D-H-MFI in this.

3.6. Postulated reaction pathway

Additional research was conducted using fresh polyether polyols, PPG, and PEG, as starting polymers, to better understand the reaction pathways. To clearly show product dispersion from pure polyol, we selected a fresh polyether polyol. Because it resembled the 3-carbon portion of the PU, PPG was chosen, whereas PEG resembled the 2-carbon portion. Using H-ZSM-5 as the catalyst, the catalytic breakdown of these compounds was examined in the same reactor configuration and under the same testing conditions. More than 90% of the polymers were transformed into liquid products, which condensed in cold methanol (−50 °C), according to mass balance calculations. Fig. 10 illustrates the product selectivity of the collected methanol. Interestingly, pure polyether polyol produced no wax, indicating that wax generation is unique to PRF and most likely caused by contaminants introduced during aminolysis. In line with results reported in the literature, polypropylene glycol was converted to propionaldehyde, acetone, and many 6-carbon dioxanes [8]. 1,4-Dioxane was the principal and highly selective decomposition product of PEG.

These observations suggest that the 3-carbon portion of PRF is the primary source of acetone and propionaldehyde, whereas the 2-carbon portion is the primary source of 1,4-dioxane. This enables the 1,4-dioxane selectivity to be estimated using PRF's ethylene oxide/propylene oxide (EO/PO) ratio. The poor selectivity to 1,4-dioxane is consistent with the ratio, which was computed from the PRF's ^{1}H NMR. These results suggest that the intrinsic EO/PO ratio of the polyether polyol used in polyurethane synthesis may influence the observed product selectivity. Based on these results, a plausible reaction pathway is hypothesized and illustrated in Fig. 11.

These findings also help clarify how wax forms during catalytic PRF cracking on zeolites. The polyurethane and aminolysis processes appear closely linked to wax production. ^{1}H NMR analysis of the collected wax indicates that it is a blend of long-chain hydrocarbons and long-chain

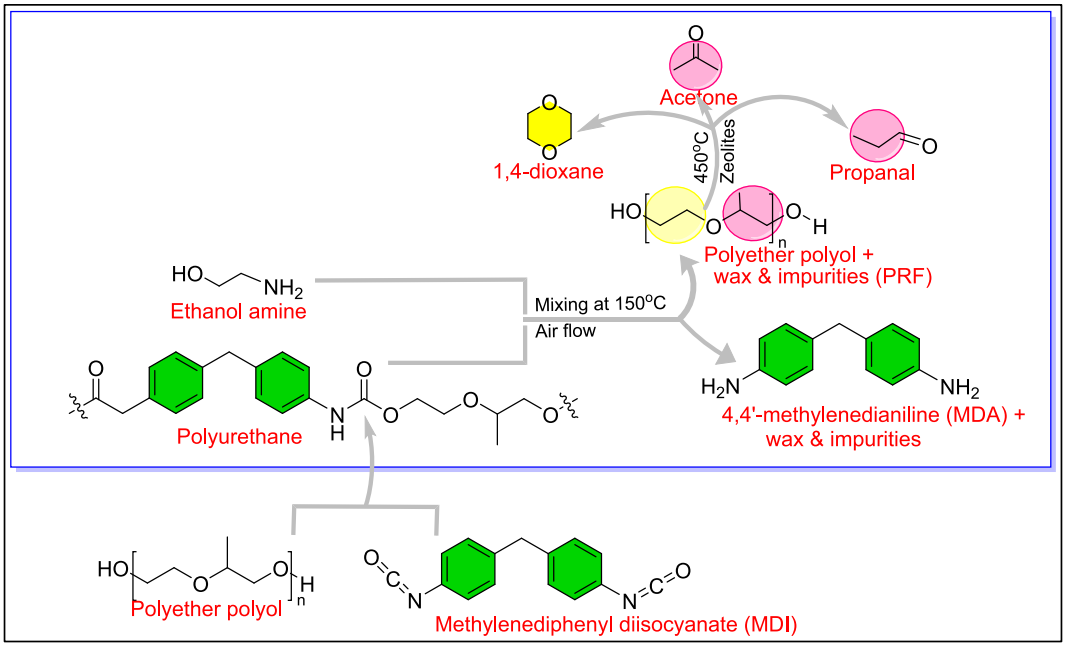


Fig. 11. Postulated PUF upcycling pathway.

ester waxes (Fig. S7). To clarify how these waxes form, more research is needed.

A small amount of airflow is required for successful separation between the PRF and the MDA-rich fraction, according to results from comparing airflow rates during operation. On the other hand, wax formation is encouraged by strong air movement. Additionally, test reactions showed that the waxes generated do not break down on zeolites at 450 °C. Such waxes were gathered and reported as a byproduct in this experiment. The literature has proposed hydrogenation processes as a means of further treating these waxes [33].

4. Conclusion

Upcycling of the commercial PUF was achieved through a two-step process: First, PU was subjected to aminolysis with MEA, and the potential effect of air on the initial cracking process was examined using DFT calculations. Based on these calculations and some limited experimental observations, we hypothesize that the presence of air may contribute to the initial cracking of PU during aminolysis. The resulting polyol-rich fraction (PRF) was subsequently used as the feedstock for catalytic cracking over 1D-shaped zeolites to produce valuable chemicals, primarily propionaldehyde. Synthesized 1D-H-MFI shows higher selectivity toward propionaldehyde (61.78 wt%) compared to a commercial H-ZSM-5 zeolite (50.25 wt%) by using 50% less amount of catalyst compared to the H-ZSM-5. Enhanced propionaldehyde selectivity correlates with the higher external surface area and reduced diffusion limitations of 1D-H-MFI, though other simultaneous changes in acidity and porosity may also play a role. Reaction pathways for PRF catalytic cracking were postulated, indicating that product distribution is possibly influenced by the EO/PO ratio of the original polyol. One possible explanation is that propionaldehyde and acetone could be related to the 3-carbon portion of the PRF, while 1,4-dioxane stems to the 2-carbon part. This study presents a potential strategy for upcycling model PU; however, further optimization, particularly regarding wax production and catalyst design, may yield even better results.

CRediT authorship contribution statement

Kanan Shikhaliyev: Writing – review & editing, Writing – original draft, Visualization, Methodology, Investigation, Formal analysis, Data curation. **Thossaporn Onsree:** Writing – original draft, Validation, Methodology, Investigation, Formal analysis. **Yusif Abdullayev:** Methodology, Investigation, Formal analysis. **Samuel M. Drummond:** Writing – review & editing, Investigation, Formal analysis. **Youngkyu Park:** Writing – review & editing, Writing – original draft, Investigation. **Alexander Katz:** Writing – review & editing, Supervision, Project administration, Funding acquisition. **Jochen Lauterbach:** Writing – review & editing, Supervision, Project administration, Funding acquisition, Conceptualization.

Declaration of competing interest

The authors declare that they have no known competing financial interests or personal relationships that could have appeared to influence the work reported in this paper.

Appendix A. Supplementary data

Supplementary data to this article can be found online at https://doi.org/10.1016/j.cej.2026.182585.

Data availability

Data will be made available on request.

References

[1] D.D. Sasu, Market volume of polyurethane worldwide from 2015 to 2022, with a forecast for 2023 to 2030. https://www.statista.com/statistics/720341/global-polyurethane-market-size-forecast/, 2023. (Accessed 22 April 2026).
[2] E.F. Kerche, L.K. Lazzari, B.F. De Bortoli, R.D. De Oliveira Polkowski, R.F.C. De Albuquerque, A systematic review of enhanced polyurethane foam composites modified with graphene for automotive industry, Graphene 2D Mater. 9 (1–2) (2024) 27–46, https://doi.org/10.1007/s41127-024-00073-x.
[3] R.V. Gadhave, S. Srivastava, P.A. Mahanwar, P.T. Gadekar, Recycling and disposal methods for polyurethane wastes: a review, Open J. Polym. Chem. 09 (02) (2019) 39–51, https://doi.org/10.4236/ojpchem.2019.92004.
[4] N.V. Gama, A. Ferreira, A. Barros-Timmons, Polyurethane foams: past, present, and future, Materials 11 (10) (2018) 1841, https://doi.org/10.3390/ma11101841.
[5] J. Oenema, H. Liu, N.D. Coensel, A. Eschenbacher, R. Van de Vijver, J. Weng, L. Li, C. Wang, K.M. Van Geem, Review on the pyrolysis products and thermal decomposition mechanisms of polyurethanes, J. Anal. Appl. Pyrolysis 168 (2022) 105723, https://doi.org/10.1016/j.jaap.2022.105723.

[6] J. Aguado, D.P. Serrano, G.S. Miguel, J.M. Escola, J.M. Rodríguez, Catalytic activity of zeolitic and mesostructured catalysts in the cracking of pure and waste polyolefins, J. Anal. Appl. Pyrolysis 78 (1) (2007) 153–161, https://doi.org/10.1016/j.jaap.2006.06.004.
[7] W.D. Woolley, Nitrogen-containing products from the thermal decomposition of flexible polyurethane foams, Br. Polym. J. 4 (1) (1972) 27–43, https://doi.org/10.1002/pi.4980040105.
[8] K. Shikhaliyev, T. Onsree, A.H. Jaeschke, S.M. Ghoreishian, K. Shariati, A. Martinez, A. Katz, S. Hwang, A. Gaffney, J.M. Urban-Klaehn, J. Lauterbach, H-ZSM-5 catalysts for the catalytic upcycling of polypropylene glycol, Appl. Catal. B Environ. 337 (2023) 122991, https://doi.org/10.1016/j.apcatb.2023.122991.
[9] C. Podara, S. Termine, M. Modestou, D. Semitekolos, C. Tsirogiannis, M. Karamitrou, A.-F. Trompeta, T.K. Milickovic, C. Charitidis, Recent trends of recycling and upcycling of polymers and composites: a comprehensive review, Recycling 9 (3) (2024) 37, https://doi.org/10.3390/recycling9030037.
[10] G. Rossignolo, G. Malucelli, A. Lorenzetti, Recycling of polyurethanes: where we are and where we are going, Green Chem. 26 (3) (2024) 1132–1152, https://doi.org/10.1039/d3gc02091f.
[11] K. Kanaya, S. Takahashi, Decomposition of polyurethane foams by alkanolamines, J. Appl. Polym. Sci. 51 (4) (1994) 675–682, https://doi.org/10.1002/app.1994.070510412.
[12] M. Ionescu, I. Mihalache, V. Zugravu, S. Mihai, S. Sever, Polyether triols, tetrahydrofuran-alkyleneoxides copolymers for flexible polyurethane foams, Cell. Polym. 14 (3) (1995) 203–229, https://doi.org/10.1177/026248931995140300 3.
[13] A.P. Gies, D.M. Hercules, A. Raghuraman, A.J. Kosanovich, M.A. Baker, S. Mukhopadhyay, I. Kobylianskii, M. Paradkar, Microstructure characterization and mechanistic insight into polyether polyols and their associated polyurethanes, Mass Spectrom. Rev. 44 (6) (2025) 889–917, https://doi.org/10.1002/mas.21862.
[14] A. Martinez, K. Shikhaliyev, X. Li, J. Han, K. Chaudhuri, S.-J. Hwang, J.M. Urban-Klaehn, A. Kuperman, A. Gaffney, J. Lauterbach, A. Katz, A multiscale investigation of polypropylene glycol polymer upcycling to propionaldehyde via catalytic cracking on acid sites of mesoporous Y zeolites, React. Chem. Eng. 9 (9) (2024) 2469–2482, https://doi.org/10.1039/d4re00001c.
[15] M.-C. Silaghi, C. Chizallet, P. Raybaud, Challenges on molecular aspects of dealumination and desilication of zeolites, Microporous Mesoporous Mater. 191 (2014) 82–96, https://doi.org/10.1016/j.micromeso.2014.02.040.
[16] W. Lutz, Zeolite Y: synthesis, modification, and properties—a case revisited, Adv. Mater. Sci. Eng. 1 (2014) (2014) 724248, https://doi.org/10.1155/2014/724248.
[17] C.K. Liu, W. Xu, Hierarchical zeolite microspheres with flat sheets, wave sheets or agglomerates induced by gemini surfactant counterion, Microporous Mesoporous Mater. 253 (2017) 160–168, https://doi.org/10.1016/j.micromeso.2017.07.002.
[18] L. Jiao, H. Xiao, Q. Wang, J. Sun, Thermal degradation characteristics of rigid polyurethane foam and the volatile products analysis with TG-FTIR-MS, Polym. Degrad. Stab. 98 (12) (2013) 2687–2696, https://doi.org/10.1016/j.polymdegradstab. 2013.09.032.
[19] H. Wang, H. Gupta, N.R. Shiju, Recycling of polyurethane waste: facile hydrothermal conversion using acidic and basic additives, ChemSusChem 19 (1) (2026) e202502372, https://doi.org/10.1002/cssc.202502372.
[20] M.J.T. D.J., G.W. Frisch, H.B. Schlegel, G.E. Scuseria, M.A. Robb, J.R. Cheeseman, G. Scalmani, V. Barone, G.A. Petersson, H. Nakatsuji, X. Li, M. Caricato, A. V. Marenich, J. Bloino, B.G. Janesko, R. Gomperts, B. Mennucci, Gaussian 16, Gaussian, Inc., Wallingford, CT, 2016.
[21] S. Grimme, J. Antony, S. Ehrlich, H. Krieg, A consistent and accurateab initioparametrization of density functional dispersion correction (DFT-D) for the 94 elements H-Pu, J. Chem. Phys. 132 (15) (2010) 154104, https://doi.org/10.1063/1.3382344.
[22] W.J. Hehre, R. Ditchfield, J.A. Pople, Self—consistent molecular orbital methods. XII. Further extensions of Gaussian—type basis sets for use in molecular orbital studies of organic molecules, J. Chem. Phys. 56 (5) (1972) 2257–2261, https://doi.org/10.1063/1.1677527.
[23] J. Tirado-Rives, W.L. Jorgensen, Performance of B3LYP density functional methods for a large set of organic molecules, J. Chem. Theory Comput. 4 (2) (2008) 297–306, https://doi.org/10.1021/ct700248k.
[24] S.C. Knight, C.P. Schaller, W.B. Tolman, M.A. Hillmyer, Renewable carvone-based polyols for use in polyurethane thermosets, RSC Adv. 3 (43) (2013) 20399–20404, https://doi.org/10.1039/C3RA44084B.
[25] M. Hashimov, Á. Kuki, T. Nagy, M. Zsuga, S. Kéki, Tandem mass-remainder analysis of industrially important polyether polyols, Polymers 12 (12) (2020) 2768.
[26] A. Nordon, C. Meunier, R.H. Carr, P.J. Gemperline, D. Littlejohn, Determination of the ethylene oxide content of polyether polyols by low-field 1H nuclear magnetic resonance spectrometry, Anal. Chim. Acta 472 (1) (2002) 133–140, https://doi.org/10.1016/S0003-2670(02)00939-X.
[27] A. Guchait, D. Maity, A.S. Sabnis, Recycling of waste polyurethane shoe sole via aminolysis route, J. Mater. Cycles Waste Manage. 26 (2) (2024) 860–871, https://doi.org/10.1007/s10163-023-01866-7.
[28] Y. Abdullayev, V. Abbasov, K. Shikhaliyev, L. Afandiyeva, J. Autschbach, Mechanistic studies on HZSM5 catalyzed polypropylene glycol conversion to propanal, in: R.A. Aliev, J. Kacprzyk, W. Pedrycz, M. Jamshidi, M.B. Babanli, F. M. Sadikoglu (Eds.), 16th International Conference on Applications of Fuzzy Systems, Soft Computing and Artificial Intelligence Tools – ICAFS-2023, Springer Nature Switzerland, Cham, 2025, pp. 157–162.
[29] R. Ramachandran, R.K. Menon, An overview of industrial uses of hydrogen, Int. J. Hydrog. Energy 23 (7) (1998) 593–598, https://doi.org/10.1016/S0360-3199(97)00112-2.
[30] W.E. Luttrell, N.P. Giles, Propylene, J. Chem. Health Saf. 23 (2) (2016) 34–36, https://doi.org/10.1016/j.jchas.2016.02.005.
[31] M. Guisnet, P. Magnoux, Deactivation by coking of zeolite catalysts. Prevention of deactivation. Optimal conditions for regeneration, Catal. Today 36 (4) (1997) 477–483, https://doi.org/10.1016/S0920-5861(96)00238-6.
[32] J. Urban-Klaehn, K. Shikhaliyev, A. Gaffney, A. Martinez, R. Zaleski, J. Lauterbach, A. Katz, A. Jaeshke, X. Li, Zeolite-based catalysts for conversion of oxygenated polymer waste by positron annihilation, ChemCatChem 16 (4) (2024) e202301282, https://doi.org/10.1002/cctc.202301282.
[33] I.-H. Choi, H.-J. Lee, G.-B. Rhim, D.-H. Chun, K.-H. Lee, K.-R. Hwang, Catalytic hydrocracking of heavy wax from pyrolysis of plastic wastes using Pd/Hβ for naphtha-ranged hydrocarbon production, J. Anal. Appl. Pyrolysis 161 (2022) 105424, https://doi.org/10.1016/j.jaap.2021.105424.